

Observability of a Sharp Majorana Transition in a Few-Body Model

Jared E. Bland*

Department of Physics & Astronomy, Purdue University, West Lafayette, IN 47907, USA

Chris H. Greene†

*Department of Physics & Astronomy, Purdue University, West Lafayette, IN 47907, USA and
Purdue Quantum Science and Engineering Institute,
Purdue University, West Lafayette, Indiana 47907, USA*

Birgit Wehefritz-Kaufmann‡

*Department of Mathematics, Purdue University, West Lafayette, IN 47907, USA
Department of Physics & Astronomy, Purdue University, West Lafayette, IN 47907, USA and
Purdue Quantum Science and Engineering Institute,
Purdue University, West Lafayette, Indiana 47907, USA*

(Dated: March 29, 2022)

We propose experimentally observable signatures for the appearance of topological Majorana quasiparticles in the few-body limit the interacting cold-atom model of [Iemini et al. Phys. Rev. Lett. 118 200404 (2017)]. In this limit, density and single-body correlations change smoothly with the model parameters. On the other hand, the calculated mutual information of opposite ends of the lattice does show a sharp transition to a non-local ground state. Furthermore, local density and parity measurements provide an experimentally viable path for observing the ground state Majorana quasiparticles in ultracold atoms. Our results lay out a promising future for utilizing few-body systems as a testing ground for Majorana physics.

The cold atom community has made remarkable strides in engineering quantum systems to exhibit many body phenomena that was formerly limited to condensed matter systems. Particularly for lattice systems exhibiting topological many-body phenomena, recent advances in engineered Hamiltonians for cold atoms have enabled large degrees of control over many-body systems [1].

Within the many-body community, there has been a wide-spread search for Majorana edge states, to find fermionic quasiparticles whose fermionic creation or annihilation operators exist as sums of two spatially separated Majorana operators, each commuting with the Hamiltonian. In Kitaev's landmark paper [2], he demonstrated that a simple mean-field model of superconductivity can exhibit these edge-mode Majoranas as quasiparticles in a quantum wire with zero excitation energy in the thermodynamic limit. For finite lattices, an energy gap proportional to e^{-L} , where L is the lattice length, is expected for spatially separated Majorana quasiparticles. Whether these zero-energy Majorana modes can truly exist in a number-conserving system and if synthetic degrees of freedom truly allow such quasiparticles to exist in a quasi-2d lattice are still open questions.

Two-body interactions drastically alter the number of possible topological phases compared to mean-field models [3]. In recent years, two groups proposed similar interacting double-wire models to exhibit Kitaev-like Majoranas in a number conserving model where a pair of wires

act as mutual particle reservoirs [4–6]. This double-wire model was then translated this into a realistic cold-atom setting in [7]. At roughly the same time, [8], proposed nearly the same model and studied the phase diagram in the many-body limit using a complementary set of parameters. In the few-body limit, several of the signatures seen in [7] survive and can be shown to emerge as the two-body interaction strength via spin-exchange is increased relative to the optical lattice tunneling rate, allowing the study of the topological phase transition from a ground state without to with Majorana quasiparticles.

In this letter, we use similar parameter values as [7] to verify the few-body limit and examine additional properties of the model, including signatures of the topological phase using quantum mutual information to indicate non-local physics. We then propose experimental signatures to contrast the topologically trivial and non-trivial phases as indicated by the mutual information, timescales to study the transition, and also investigate properties of the low-lying states and consistency with finite-energy Majorana ground state quasiparticles in this limit.

The model of Iemini et al. has a basis that is composed of four hyperfine states of a fermionic alkaline earth-like atom [9], physically labeled according to an orbital angular momentum quantum number (labeled $p = \pm$) and pseudo-spin (labeled $\alpha = \uparrow, \downarrow$), with couplings between two effective nuclear spin states and two orbital spin states provided by interactions with the photon field of the optical lattice as well as two-body interactions between the atoms [10–12]. The Iemini Hamiltonian is constructed from a sum of a nearest-neighbor tunneling, onsite potential, synthetic spin-orbit coupling, and a two-

* bland3@purdue.edu

† chgreene@purdue.edu

‡ ebkaufma@purdue.edu

body spin-exchange interaction:

$$H_I = \sum_j H_{T,j} + H_{U,j} + H_{SO,j} + H_{W,j}.$$

The single site tunneling terms are given by

$$H_{T,j} = \sum_{p,\alpha} T(a_{\alpha,p,j+1}^\dagger a_{\alpha,p,j} + \mathcal{H.C.}).$$

The local on-site diagonal interaction is composed of terms

$$H_{U,j} = U_+ n_{\uparrow,+1,j} n_{\downarrow,+1,j} + U_- n_{\downarrow,-1,j} n_{\uparrow,-1,j} \\ + U \sum_{\alpha,\beta} (n_{\alpha,-1,j} n_{\beta,+1,j}).$$

In recent years, spin-orbit coupling has become feasible using synthetic magnetic fields [13–15]. The spin-orbit terms may be written as

$$H_{SO,j} = (b + \alpha_R)(a_{\uparrow,+1,j}^\dagger a_{\downarrow,-1,j+1} + a_{\uparrow,-1,j}^\dagger a_{\downarrow,+1,j+1} + \mathcal{H.C.}) \\ + (b - \alpha_R)(a_{\uparrow,+1,j+1}^\dagger a_{\downarrow,-1,j} + a_{\uparrow,-1,j+1}^\dagger a_{\downarrow,+1,j} + \mathcal{H.C.}),$$

where the time-reversal symmetry breaking coefficients $b \pm \alpha_R$ describe the sum and difference of an effective Zeeman-splitting term b that is spatially uniform in this approximation and a Rashba velocity α_R , providing an analogous effect to an external magnetic field. The final term, a two-body scattering term related to spin-exchange [16, 17], is given by

$$H_{W,j} = W(a_{\uparrow,+1,j}^\dagger a_{\downarrow,-1,j}^\dagger a_{\downarrow,+1,j} a_{\uparrow,-1,j} + \mathcal{H.C.}).$$

With these interactions, the Hamiltonian may be written in a two-block diagonal form according to a suitable parity operator. We propose a slightly different parity operator from the original paper [7], whose definition needs modification for odd total particle number. In analogy with [4], a study of a double-wire model, fermions of species $(\uparrow, +)$ and $(\downarrow, -)$ at site j are analogous to adjacent-site single species fermions in the upper wire of the double-wire model. With this, we may define two reasonable parity measurements, P_+ and P_- :

$$P_+ = \left(\sum_j n_{\uparrow,+1,j} + n_{\downarrow,-1,j} \right) \bmod 2, \text{ and} \quad (1)$$

$$P_- = \left(\sum_j n_{\uparrow,-1,j} + n_{\downarrow,+1,j} \right) \bmod 2. \quad (2)$$

Importantly, for even particle number, these two definitions are equivalent, but exchange the meaning of even- and odd-parity of [7]. For odd lattice fillings, P_+ and P_- define even- and odd-parities in the opposite manner. For this paper, we use the definition P_+ .

The Hamiltonian has a chiral symmetry that leaves the Hamiltonian invariant: $a_{\alpha,p,j}^{(\dagger)} \mapsto a_{-\alpha,p,L-j}^{(\dagger)}$. For even

numbered fillings, this symmetry commutes with the degenerate parity operators. In lattices with odd total occupation number, however, the chiral transformation exchanges the parity sector of a state for every eigenstate of the parity operator. Thus, for all parity eigenstates with odd total particle number, the energy spectrum is at least doubly degenerate due to the chiral symmetry relationship between states in opposite parity sectors. For even total numbered states, the \mathbb{Z}_2 symmetry from the generalized notion of parity commutes with the chiral transformation, and the states are not identically degenerate. When $U_\pm, U = 0$, there is an additional symmetry $a_{\alpha,p,j}^{(\dagger)} \mapsto a_{-\alpha,-p,j}^{(\dagger)}$ that simultaneously commutes with the chiral transformation as well as the parity operator, and so does not place any additional constraints on the spectrum irrespective of the particle number. For comparison with the thermodynamic limit, the filling fraction of N atoms on an L site lattice $\lambda = N/4L = 1/4$ is used since, in the few-body limit, this ratio is the simplest for comparisons with the thermodynamic limit to have an integer filling for all lattice length sizes. Finite-size effects prevents simple comparison with different filling fractions away from this fraction.

For the remainder of this paper, we set $T = -1$ and consistently use W/T in figures to emphasize that T sets the energy scale used, and further set $(U_\pm, U, b + \alpha_R, b - \alpha_R) = (0, 0, 8, 0)$ to utilize similar parameters as [7] with $L = 7 = N$ in the even parity sector. W/T is varied to study the transition from the non-topological regime with no edge modes to the topological regime with edge-state physics.

In agreement with their bosonization, outside the crossover region of $W/T \in (11, 14)$ we see four low energy states that are nearly degenerate in energy in the in Fig. 1. In the few-body limit, the transition regime is spread out over a large set of parameter values due to finite-size effects. In the strong-coupling limit of few-body regime, the states separate into bands with two nearly degenerate eigenvalues corresponding to the spin-wave excitation in the effective orbital degree of freedom over a large parameter range.

Our few-body calculations show strong qualitative agreement with [7]. For $W/T = 16$, the ground state single species correlators $\langle a_{\uparrow,+1,j}^\dagger a_{\uparrow,-1,j} \rangle$, which measure the intra-species correlation of the first site with another site j , initially decay then rebound exponentially, see Fig. 2 (b). On the other hand, the non-topological low-energy states decay exponentially with no rebounding, as shown in Fig. 2 (a) for $W = 10T$ as well as the non-topological excited states with of Fig. 2 (b). The single species correlations indicate long-range correlation as W/T is increased but do not change abruptly, making it difficult to pinpoint the location of the phase transition using the single-particle correlations as the sole signature of the transition in the few-body limit.

The mutual information is a signature that shows the topological phase transition when the chiral symmetry protects the topological properties of the ground state

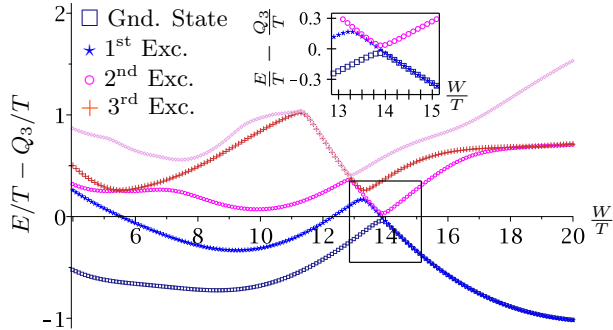


FIG. 1. The lowest energy eigenvalues of the even parity sector, shifted so that the center of the the low-lying energies is approximately zero by subtracting a cubic fit of the average of the first four energies $Q_3(x) = 0.0016x^3 - 0.1303x^2 + 0.8999x - 64.131$, as W/T is varied. During the crossover from non-topological to topological phase, a zoo of states is formed and we can see the four-lowest states separate, with the ground state becoming approximately (doubly) degenerate. (Color online) We use the same color scheme for all plots. *Inset:* There is an avoided crossing between the lowest energy state and the second excited state. When $U = 0 = U_{\pm}$, the Hamiltonian may be written in a four-block diagonal basis, and there is a non-avoided crossing of an eigenvector in another symmetry sector.

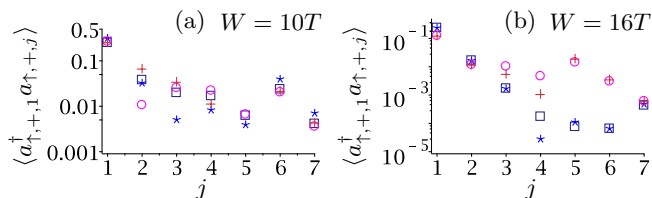


FIG. 2. Single species correlators $\langle a_{\uparrow,+1}^\dagger a_{\uparrow,+j} \rangle$ for the low energy states for $(L, N, T, U, \alpha_R, b) = (7, 7, -1, 0, 4, 4)$. (a) In the trivial phase ($W = 10T$), all low-energy states exhibit a staggered decay with no rebounding of single-particle correlations. (b) In the topological phase ($W = 16T$) the degenerate ground state manifold exhibits exponential decay and rebounding on the other end of the chain while the trivial states do not exhibit correlations that rebound. As W is increased in magnitude, the bulk continues to lose correlation with the edges.

in this system. The mutual information of two quantum systems A, C is the relative von Neumann entropy between their joint reduced density matrix and the tensor product of their individual reduced density matrices: $I(A : C) = S_A + S_C - S_{AC}$ [18, 19]. In the case of a pure state in a quantum system across regions A, B, C , we may write this as $I(A : C) = S_A + S_C - S_B$, where S_X is the von Neumann entropy of the state's reduced density matrix over region X [20]. Fig. 3 contains a sample 7 site lattice divided into regions A, B, C for various sizes of the regions, with $L_A = L_C$ given in the drawing's

annotation. For the case of $N = 7$, the chiral symmetry guarantees that the entanglement spectra in the center of the lattice are identical in the even and odd parity ground states (similar to [21]'s inversion symmetry analysis of a mean-field model), but the mutual information displays a sharp transition as W/T is increased when subsystems A and C comprise 1 site each. For larger regions of A, C , the increase of W/T does not cause as sharp a change of the mutual information between subsystems A and C since the “bulk” (region B) is providing most of the entanglement across the division using short-ranged entanglement, which varies smoothly with parameters, as shown in Fig. 4. Thus, the mutual information gives insight into the interplay between the length scales of edge-modes and short-ranged bulk entanglement even in the presence of additional symmetries that prevent the analysis using the entanglement spectra in opposite parity sectors.

7 Site Lattice with Several Sample Divisions

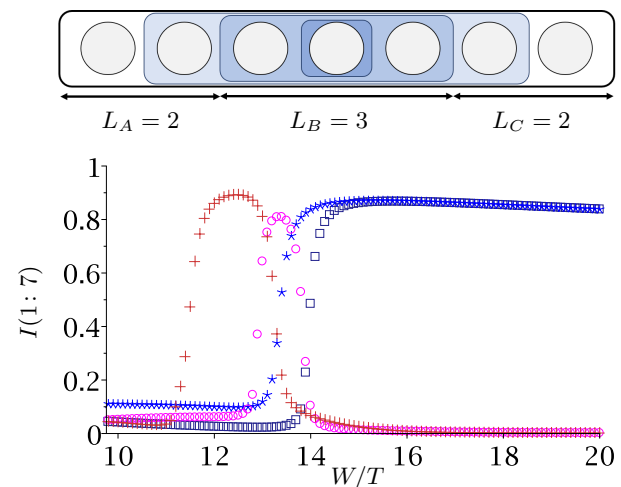


FIG. 3. *Top:* Sample lattice with division into three regions A, B , and C . *Bottom:* Mutual information between the first and last sites ($L_A = 1 = L_C$) for the four low-energy states as W/T is varied. The degenerate ground state manifold has topological properties after the transition region $W/T \in [11, 14]$, while the first excited state manifold has no edge-edge correlation beyond a product state.

While the mutual information provides a sharp theoretical understanding of the non-local nature of the ground state manifold in the topological regime, it is not experimentally measurable since it is non-linear in the density matrix. More importantly, even though it provides a measure of non-local physics by integrating out the “bulk” center region of the lattice, it does not give direct insight into any quasiparticle properties of the ground state aside from non-local entanglement. In addition to the single particle Green functions of Fig. 2 (a)-(b), we propose two additional experimental signatures distinguishing the topological and non-topological regimes of the model: the density expectation values

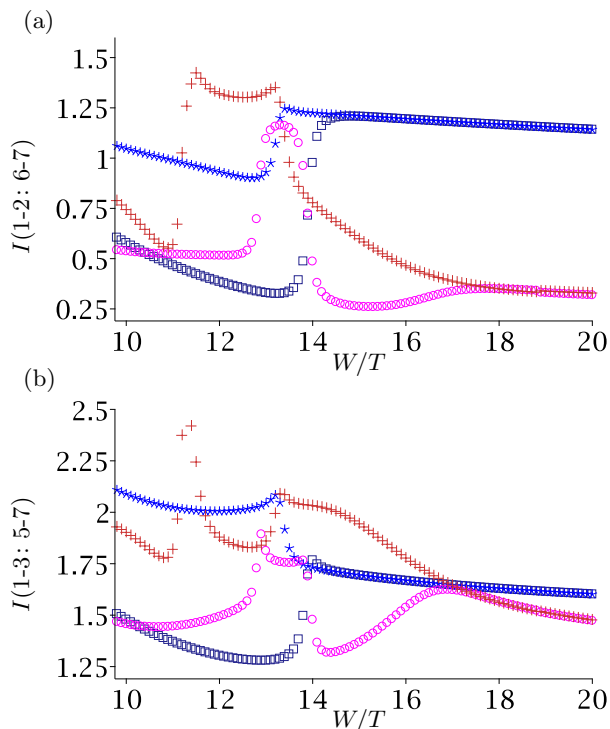


FIG. 4. Mutual information of the left and right edges for (a) $L_A = 2$ and (b) $L_A = 3$. As the boundaries for the mutual information calculation are increased, we can see the transition towards bulk behavior as short-ranged entanglement provides the majority to the entanglement between the two halves.

across the lattice and local parity measurements.

The density expectation value $\langle n_{\uparrow,+j} \rangle$ distinguishes between topological and non-topological states when varying W/T . Below the transition threshold (indicated by the change in the mutual information), all four fermionic species have nearly 0 density at one end of the lattice or the other for all low-energy eigenvectors, exemplified in Fig. 5 (a) with $W/T = 10$. Then, when the mutual information indicates a delocalized mode, the densities at both ends are comparable, with $W/T = 16$ in Fig. 5 (b) giving a characteristic example.

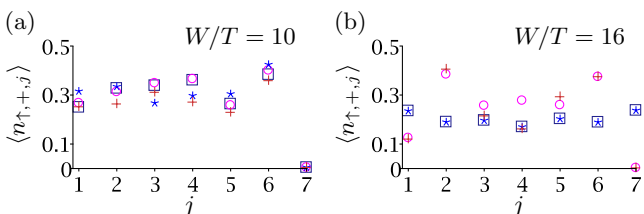


FIG. 5. (a) In the trivial regime of the model ($W = 10T$ in this plot), all low-energy states have very low densities at one edge of the lattice for each particle species. (b) In the topological regime ($W = 16T$), the densities of the topological ground state manifold have a comparable values on both ends of the lattice, while the non-topological excited states maintain near-zero edge densities at one end of the lattice.

A sharp few-body experimental signature of the proposed Majorana mode is provided by the parity operator restricted to the first L_A sites on the left-hand side of the lattice: $P_{+,L_A} = (\sum_{j=1 \dots L_A} n_{\uparrow,+j} + n_{\downarrow,-j}) \bmod 2$. Since two spatially separated Majorana modes each locally break parity, but conserve it globally, we may look at the expectation value of the operator while keeping $L_A < L/2$. With only 7 sites, this signature provides evidence of edge parity breaking while maintaining global parity. In the even parity sector, the parity expectation on the left- and right-hand sides of any cut are identical (to cancel and give 0 as the global parity measurement). The even parity ground state sharply changes in its parity expectation value for the left-hand side, as shown in Fig 6, which plots $\langle P_{+,L_A} \rangle$ of the even parity ground state for $L_A = 1, 2, 3$. This sharp transition of the left-hand side parity measurement while fixing the global parity gives a sharp experimental signature of a topological mode strongly consistent with Majorana quasiparticles in the ground state.

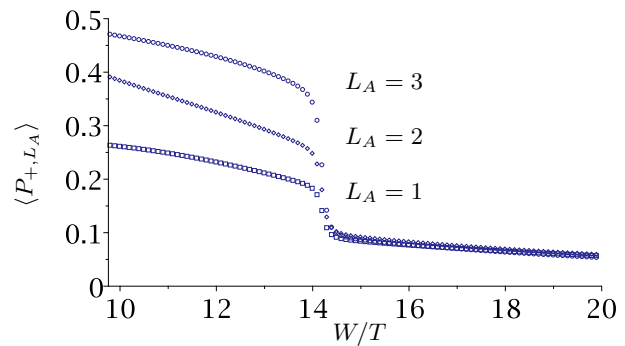


FIG. 6. Local ground state parity measurements of the left-hand side $\langle P_{+,L_A} \rangle$ plotted for $L_A = 1, 2, 3$ in the even parity sector. With just a single site, the local parity measure shows a small but noticeable transition, while the local parity of the first three sites provides a very strong evidence of the phase transition.

The presence of avoided crossings of the energy levels in Fig. 1, as a function of the parameter W/T in the Hamiltonian, suggests a way to experimentally create the topological phase possessing Majorana character, starting from the non-topological phase. Specifically, begin by preparing the system in the lowest energy level to the left of the avoided crossing, i.e. at $W/T \ll 13.9$. Then by sweeping at a sufficiently slow ramp to $W/T \gg 13.9$, the system will transition into the topological Majorana phase with a controllable high probability. The requisite ramp speed to stay in the lowest energy level through this avoided crossing can be estimated from Fig. 1 using the Landau-Zener model [22]. For definiteness, we consider a scenario where the tunneling term is fixed at $T = 100$ h Hz, while W is swept through the value $13.9T$ at a linear temporal ramp rate dW/dt . Then the Landau-Zener formula gives the probability to remain in the lower branch of the avoided crossing to be

$\mathcal{P} = 1 - \exp(-2\pi\Gamma)$, where $\Gamma = \Delta^2/\hbar/(4|dE_2/dW - dE_1/dW/dt|)$. Our calculation of the critical value of the ramp rate for which the adiabatic transition occurs with 50% probability is $(dW/dt)_{\text{crit}} = 1360$ h Hz/s, i.e. $\Gamma = (0.110 \times 1360 \text{ h Hz/sec})/dW/dt$. Thus a ramp speed of 136 h Hz/s keeps the system on the lower branch and produces the topological Majorana phase with 99.9% probability. For Yb, the lifetime of the excited electronic states ($\sim 10^2$ sec) is far longer than the time to sweep through a change of W of 1000 h Hz with the slow ramping rate of 136 h Hz/sec [13, 14]. The long-lived states along with the Landau-Zener analysis gives experimentalists a wide variety of control over the transition from the non-topological phase to the topological Majorana phase.

We have discussed the symmetries and corresponding operators of the interacting model of [7] and proposed a different parity definition in analogy with [4]. Furthermore, we have demonstrated the utility of mutual information as a way to complement entanglement spectra for categorizing topological phase in the presence of additional symmetries. The mutual information along

with the local parity measurement in the ground state supports the conclusion of [7] that as the two-body scattering is increased, edge modes consistent with Majorana quasiparticles appear in the ground state.

Future work will yield more insight into the characteristics of the edge state physics. Theoretically, further study of the transition region will may calculate the length scales of the Majorana quasiparticles in the low-energy physics. The experimental signatures proposed here focus on local density measurements, which are standard in the measurements used by ultracold atomic experimental groups and are accessible to groups studying these alkaline earth-like atoms [13–17, 23–25]. In the few-body limit of only 7 sites and 7 particles, our results suggest that in the topological regime there is a degenerate ground state manifold with edge Majorana characteristics separated by a gap to the non-topological excited states.

We would like to thank Nima Lashkari for many helpful discussions on quantum information theory. This work has been partially supported by NSF PHY-1255409 (J.E.B. and B.W.-K.) and NSF PHY-1912350 (C.H.G.).

-
- [1] N. R. Cooper, J. Dalibard, and I. B. Spielman, Topological bands for ultracold atoms, *Rev. Mod. Phys.* **91**, 015005 (2019).
- [2] A. Y. Kitaev, Unpaired majorana fermions in quantum wires, *Pyhsics-Uspekhi* **44**, 131 (2001).
- [3] L. Fidkowski and A. Kitaev, Effects of interactions of the topological classification of free fermion systems, *Phys. Rev. B* **81**, 134509 (2010).
- [4] N. Lang and H. P. Büchler, Topological states in a microscopic model of interacting fermions, *Phys. Rev. B* **92**, 041118(R) (2015).
- [5] K. Guther, N. Lang, and H. P. Büchler, Ising anyonic topological phase of interacting fermions in one dimensions, *Phys. Rev. B* **96**, 121109(R) (2017).
- [6] F. Iemini, L. Mazza, D. Rossini, R. Fazio, and S. Diehl, Localized majorana-like modes in a number-conserving setting: An exactly solvable model, *Phys. Rev. Lett.* **115**, 156402 (2015).
- [7] F. Iemini, L. Mazza, L. Fallani, P. Zoller, R. Fazio, and M. Dalmonte, Majorana quasiparticle protected by \mathbb{Z}_2 angular momentum conservation, *Phys. Rev. Lett.* **118**, 200404 (2017).
- [8] X. Zhou, J.-S. Pan, Z.-X. Liu, W. Zhang, W. Yi, G. Chen, and S. Jia, Symmetry-protected topological states for interacting fermions in alkaline-earth-like atoms, *Phys. Rev. Lett.* **119**, 185701 (2017).
- [9] C. He, E. Hajiyev, Z. Ren, B. Song, and G. Jo, Recent progresses of ultracold two-electron atoms, *J. Phys. B: At. Mol. Opt. Phys.* **52**, 102001 (2019).
- [10] N. Goldman, G. Jüzeliunas, P. Öhberg, and I. B. Spielman, Light-induced gauge fields for ultracold atoms, *Rep. Prog. Phys.* **77**, 126401 (2014).
- [11] R. Zhang, Y. Cheng, P. Zhang, and H. Zhai, Controlling the interaction of ultracold alkaline-earth atoms, *Nat. Rev. Phys.* **2**, 213220 (2020).
- [12] S.-L. Zhang and Q. Zhou, Manipulating novel quantum phenomena using synthetic gauge fields, *J. Phys. B: At. Mol. Opt. Phys.* **50**, 222001 (2017).
- [13] M. L. Wall, A. P. Koller, S. Li, X. Zhang, N. R. Cooper, J. Ye, and A. M. Rey, Synthetic spin-orbit coupling in an optical lattice clock, *Phys. Rev. Lett.* **116**, 035301 (2016).
- [14] S. Kolkowitz, S. L. Bromley, T. Bothwell, M. L. Wall, G. E. Marti, A. P. Koller, X. Zhang, A. M. Rey, and J. Ye, Spin-orbit coupled fermions in an optical lattice clock, *Nature* **542**, 66 (2017).
- [15] L. F. Livi, G. Cappellini, M. Diem, L. Franchi, C. Clivati, M. Frittelli, F. Levi, D. Calonico, J. Catani, M. Inguscio, and L. Fallani, Synthetic dimensions and spin-orbit coupling with an optical clock transition, *Phys. Rev. Lett.* **117**, 220401 (2016).
- [16] L. Riegger, N. Darkwah Oppong, M. Höfer, D. R. Fernandes, I. Bloch, and S. Fölling, Localized magnetic moments with tunable spin exchange in a gas of ultracold fermions, *Phys. Rev. Lett.* **120**, 143601 (2018).
- [17] F. Scazza, C. Hofrichter, M. Höfer, P. C. D. Groot, I. Bloch, and S. Fölling, Observation of two-orbital spin-exchange interactions with ultracold $su(n)$ -symmetric fermions, *Nature Physics* **10**, 779784 (2014).
- [18] M. Wilde, *Quantum Information Theory* (Cambridge University Press, 2017).
- [19] M. A. Nielsen and I. L. Cheung, *Quantum Computation and Quantum Information* (Cambridge University Press, 2012).
- [20] C. Navarrete-Benlloch, *An Introduction to the Formalism of Quantum Information with Continuous Variables* (Morgan & Claypool Publishers, 2015).
- [21] A. M. Turner, F. Pollmann, and E. Berg, Topological phases of one-dimensional fermions: An entanglement point of view, *Phys. Rev. B* **83**, 075102 (2011).
- [22] H. Nakamura, *Nonadiabatic Transition: Concepts, Basic*

Theories, and Applications (World Scientific, 2012).

- [23] F. A. An, E. J. Meier, and B. Gadway, Direct observation of chiral currents and magnetic reflection in atomic flux lattices, *Science Advances* **3**, e1602685 (2017).
- [24] D. Okunoa, Y. Amano, K. Enomoto, N. Takei1, and Y. Takahashi, Schemes for nondestructive quantum gas microscopy of single atoms in an optical lattice, *New J. Phys.* **22**, 013041 (2020).
- [25] Y. Takata, S. Nakajima, J. Kobayashi, K. Ono, Y. Amano, and Y. Takahashi, Current-feedback-stabilized laser system for quantum simulation experiments using yb clock transition at 578 nm, *Rev. Sci. Instrum.* **90**, 083002 (2019).